Catal Lett (2008) 122:330–337
DOI 10.1007/s10562-007-9383-3

An Efficient and Reusable Catalyst of Bismuth-Containing SBA-15 Mesoporous Materials for Solvent-free Liquid Phase Oxidation of Cyclohexane by Oxygen

Huanling Wang · Rong Li · Yunfeng Zheng · Hangning Chen · Fushan Wang · Jiantai Ma

Received: 8 June 2007 / Accepted: 9 December 2007 / Published online: 3 January 2008

Abstract Bismuth-containing SBA-15 mesoporous materials with different n_{si}/n_{Bi} ratio was synthesized for the first time through a direct hydrothermal method, and characterized by various physico-chemical techniques. XRD patterns indicate that the synthesized materials have an ordered two-dimensional *p6mm* hexagonal mesostructure. Transmission electron microscopy and scanning electron microscopy studies show that Bi-SBA-15 has well-ordered hexagonal arrays of mesoporous channels and the morphology of rod-like particles. Raman spectroscopy and UV–Vis DRS show that bismuth atoms in Bi-SBA-15 exist in a highly dispersed state, and locate mainly at tetrahedrally coordinated sites. Thermogravimetric analysis was used to observe the removal of the organic template P_{123}. In the catalytic test, Bi-SBA-15 is found to be a very efficient and reusable catalyst for the oxidation of cyclohexane, in a solvent-free system, with oxygen as oxidant. The influence of different parameters, such as reaction time, reaction temperature, oxygen pressure, and the dosage of catalyst on the oxidation of cyclohexane, is also investigated.

Keywords Bi-SBA-15 · Cyclohexane oxidation · Oxygen · Solvent-free

1 Introduction

The selective oxidation of cyclohexane is an industrially important reaction, because its oxidation products, viz., cyclohexanol and cyclohexanone, are important intermediates in the production of adipic acid and caprolactam, which are used to manufacture nylon-6 and nylon-66 polymers [1, 2]. In the present industrial process, cyclohexane conversion is lower than 5%, and the total selectivity of cyclohexanone and cyclohexanol is lower than 80%. Therefore, the great demand for these oxidation products and the increased environmental concerns call for a more effective catalytic process using heterogeneous catalysts and environmentally friendly oxidants. Among the commonly used oxidants, molecular oxygen is the cheapest and cleanliest oxidant. Catalytic liquid phase oxidation of cyclohexane by oxygen in the absence of solvents and additives is the most attractive. Although great efforts have been made to this reaction, it continues to be a challenge [3–10].

In recent years, redox molecular sieves have been studied extensively as catalysts for cyclohexane oxidation using oxygen as oxidant in a solvent-free system [11–20]. SBA-15 mesoporous molecular sieves, synthesized by Zhao et al. in 1998, have attracted considerable attention due to its tunable pore diameter, thicker walls, high hydrothermal stability and potential applications in a wide variety of fields [21]. Various metal heteroatoms, such as Cr [22], Mn [23], Ti [24, 25], Fe [26], Zr [27], Ga [28, 29], Al [30, 31], and V [32], have been incorporated in the framework of SBA-15, and most of them have been tested for their catalytic activities in a certain reaction. According to the literatures, metal heteroatom-containing aluminophosphate, ZSM-5, MCM-41, MCM-48 or small pore mesoporous silica has been used as catalyst for cyclohexane oxidation [11–20]. However, to the best of our knowledge, no research has been reported on using heteroatom-incorporated SBA-15 as catalyst for the selective oxidation of cyclohexane with O_2 in a solvent-free system.

H. Wang · R. Li · Y. Zheng · H. Chen · F. Wang · J. Ma (✉)
College of Chemistry and Chemical Engineering,
Lanzhou University, Lanzhou 730000, P.R. China
e-mail: majiantai@lzu.edu.cn

In the present study, we report an efficient procedure for the selective oxidation of cyclohexane in a solvent-free system using O_2 as oxidant and bismuth-containing SBA-15 as catalyst, which was synthesized, for the first time, by a direct hydrothermal method and characterized by ICP, XRD, transmission electron microscopy (TEM), scanning electron microscopy (SEM), UV–Vis DRS, Raman spectroscopy and thermogravimetric (TG) analysis. The influence of different parameters, such as reaction time, reaction temperature, oxygen pressure and the dosage of catalyst on the oxidation of cyclohexane, is also investigated in detail.

2 Experimental

Bi-SBA-15 was prepared as follows: 2 g P_{123} was dissolved in 12.5 mL water to get a clear solution. Thereafter, the required amount of dilute HCl solution was added, and the solution was stirred for another 1 h to be associated with the hydronium ions with the alkylene oxide units. Then, 4.25 g TEOS and the required amount of $Bi(NO_3)_3$ solution (Si/Bi = 20, 30, 50, 70 in molar ratio) were added, and the resulting mixture was stirred for 24 h at 313 K. Then it was transferred into an autoclave to crystallize for 24 h at 373 K under static conditions. The resulting solid was filtered, washed several times with water and dried overnight at 373 K. The molar gel composition was 1 TEOS/0.014–0.05 $Bi(NO_3)_3$/0.017 P_{123}/3.65 HCl/203 H_2O. Finally, the solid was calcined at 823 K in air for 6 h to remove the template completely. According to the different bismuth content in the Bi-SBA-15 (analyzed by ICP), the catalysts were labeled A, B, C, D. For comparisons, pure siliceous SBA-15 was also synthesized according to [21].

The content of Bi was quantified by inductively coupled plasma emission spectroscopy (ICP) on a *Rigaku JY38S* ICP-AES spectrometer. XRD patterns were recorded on a *Rigaku D/Max-2400* diffractometer using Cu Kα radiation ($\lambda = 0.15418$ nm) in the 2θ range of 0.5–10°. TEM measurements were taken on a *Jeol-JEM-100* electron microscope. SEM measurements were taken on a *JSM-5600LV* electron microscope. Raman spectra were measured on a *Nicolet Raman-910* spectrometer. UV–Vis spectra were measured on a *Shimadzu UV-240* spectrometer. The TG analysis was carried out on a *Dupont-1090* TG analyzer in flowing air at a heating rate of 10 K/min.

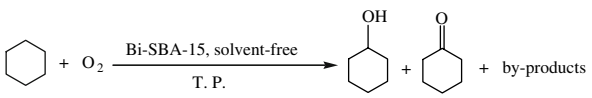

In a typical reaction procedure, 8 mL (74 mmol) cyclohexane and Bi-SBA-15 catalyst were added to a 100 mL stainless steel reactor, equipped with a magnetic stirrer and an automatic temperature controller. The reactor was flushed three times with O_2 and pressurized to the desired pressure, then heated to the desired temperature with stirring. After reaction, the reactor was cooled to room temperature and slowly depressurized. Then, a suitable quantity of acetone was added into the reactor to dissolve the products. The quantitative analyses of the liquid samples were carried out by GC (*P.E. AutoSystem XL*) with a SE-54 capillary column and an FID detector, using chlorobenzene as an internal standard. The identity of the components was verified by GC-MS (*Agilent 6890N/5973N*). It is essential that the samples were doubly analyzed by GC, before and after reducing cyclohexyl hydroperoxide (CHHP, the first and indispensible oxygenated product of cyclohexane oxidation) to cyclohexanol with triphenylphosphine [33]. As CHHP partially decomposes upon injection to form some cyclohexanol and cyclohexanone, an appreciable positive deviation for quantifying cyclohexanol and cyclohexanone could be caused while the samples were directly analyzed by GC. A blank cyclohexane oxidation reaction over SBA-15 was also performed under the same reaction conditions.

In order to confirm the possible mechanism, the reaction was carried out in the presence of small quantity of radical initiator *tert*-butylhydroperoxide (TBHP, 3 wt% of cyclohexane) or radical inhibitor hydroquinone (HQ, 3 wt% of cyclohexane).

3 Results and Discussion

3.1 Catalyst Characterization

Low-angle X-ray diffraction is the first and foremost technique to confirm the formation of mesophase. Figure 1 illustrates the low-angle powder XRD patterns of the Bi-SBA-15 samples synthesized with different Si/Bi ratio. The parent SBA-15 and the Bi-SBA-15 samples all show three well-resolved diffraction peaks in the 2θ range of 0.5–2°, which correspond to (100), (110), and (200) reflections. The XRD patterns match well with the pattern reported for SBA-15 [21], indicating that the synthesized materials have an ordered two-dimensional (2D) *p6mm* hexagonal mesostructure.

Table 1 lists the d_{100} spacing and hexagonal unit-cell parameter (a_0) [calculated from (100) peak]. As shown in Table 1, the unit-cell parameter of Bi-SBA-15 samples is found to be higher than that of parent SBA-15, and it increases significantly with the increase of Bi content. Such expansion of the unit-cell parameter indicates the successful incorporation of Bi in the framework. Expansion of

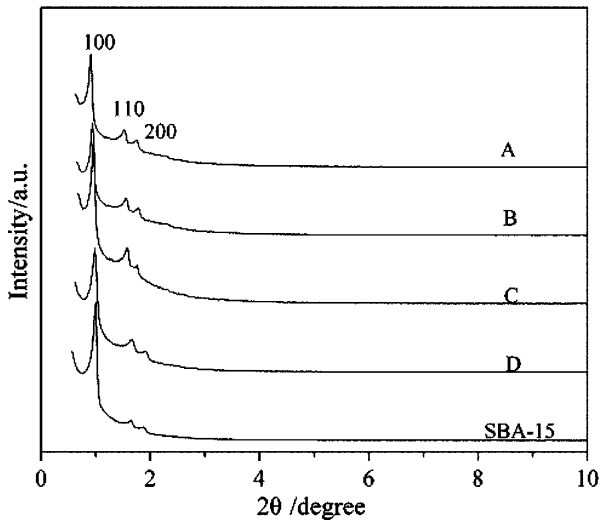

Fig. 1 The XRD patterns of SBA-15 and Bi-SBA-15 catalysts with different Bi content: (**A**) 1.87 wt%, (**B**) 1.22 wt%, (**C**) 0.76 wt%, (**D**) 0.47 wt%

Table 1 Analytic data of Bi-SBA-15 samples

Sample	Si/Bi gel	Bi content (wt%)	d_{100} (Å)	a_0^a (Å)
A	20	1.87	98.84	114.13
B	30	1.22	94.94	109.63
C	50	0.76	92.83	107.19
D	70	0.47	90.37	104.35
SBA-15	–	–	89.66	103.53

[a] a_0 the lattice parameter calculated from XRD data using the formula $a_0 = 2d_{100}/\sqrt{3}$.

the unit-cell parameter was also observed before for Ga-SBA-15 and Ti-SBA-15 [28, 29, 34].

As shown in Fig. 2, the TEM image of Bi-SBA-15 (D) shows well-ordered hexagonal arrays of mesoporous channels, further confirming that the Bi-SBA-15 sample has a 2D *p6mm* hexagonal structure. The distance between two consecutive centers of hexagonal pores estimated from the TEM images is about 11 nm, and the pore diameter is about 6 nm.

Scanning electron microscopy is used to determine the particle size and particle morphology of the synthesized sample. As shown in Fig. 3, Bi-SBA-15 (B) has the morphology of rod-like particles, with a relatively uniform size of ca. 0.4 μm in width and 0.8–1.1 μm in length.

Figure 4 shows the Raman spectra for Bi-SBA-15 and crystalline Bi_2O_3. Crystalline Bi_2O_3 is a very strong Raman scatterer, so the absence of intense peaks at ca. 2136, 1724, 1410, 449, and 315 cm^{-1} (in Bi_2O_3) indicates that the bismuth is highly dispersed in the silica-based framework structure.

UV–Vis DRS is extensively used to detect the framework and extra-framework metal species in molecular

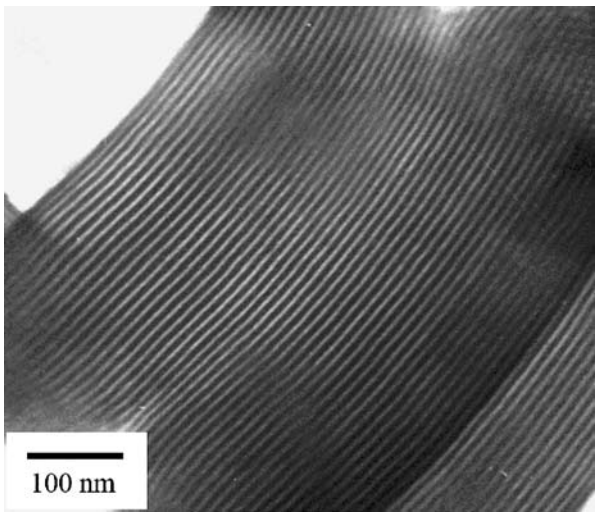

Fig. 2 TEM images of Bi-SBA-15 (D)

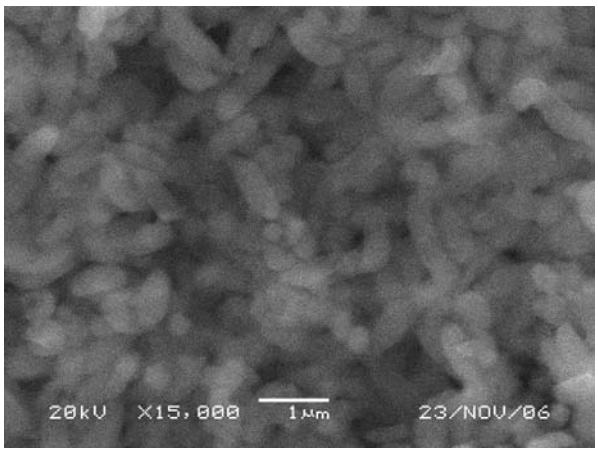

Fig. 3 SEM images of Bi-SBA-15 (B)

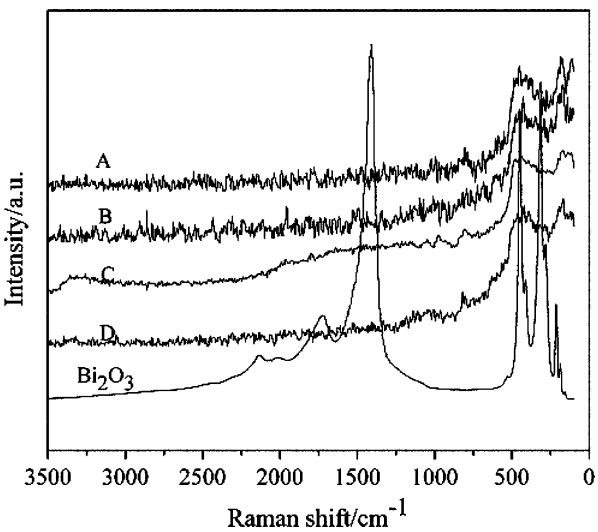

Fig. 4 Raman spectra for the Bi-SBA-15 catalysts and Bi_2O_3: (**A**) 1.87 wt%, (**B**) 1.22 wt%, (**C**) 0.76 wt%, (**D**) 0.47 wt%

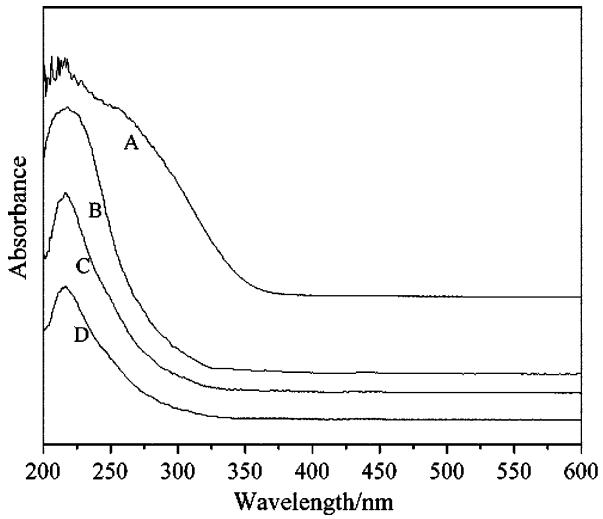

Fig. 5 UV–Vis spectra for the Bi-SBA-15 catalysts: (**A**) 1.87 wt%, (**B**) 1.22 wt%, (**C**) 0.76 wt%, (**D**) 0.47 wt%

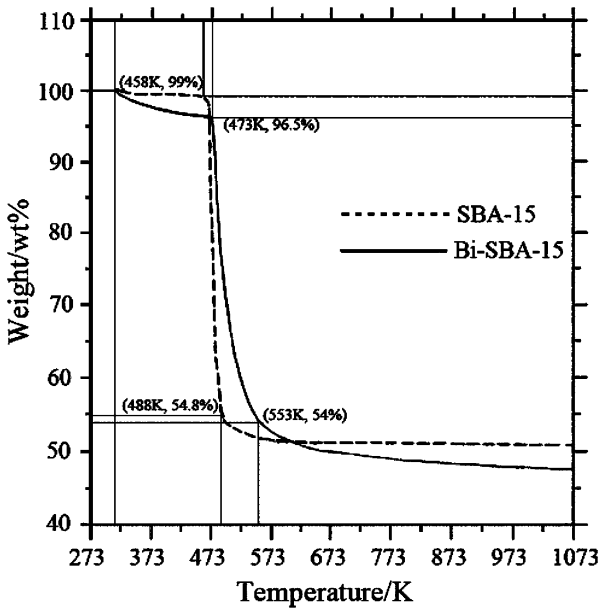

Fig. 6 Thermogravimetric analysis profiles of SBA-15 and Bi-SBA-15 (B)

sieves [35]. As shown in Fig. 5, the diffuse-reflectance UV–Vis spectra for Bi-SBA-15 samples with Si/Bi = 20, 30, 50, and 70 show a ligand-to-metal charge transfer (from an O^{2-} to an isolated Bi^{3+} ion in a tetrahedral configuration) band at about 215 nm, indicating the presence of tetrahedral isolated Bi^{3+} ion in the SBA-15 mesoporous framework. Whereas a small shoulder band at about 250 nm is observed for the sample having Si/Bi ratio of 20, which may indicate the presence of hexa-coordinated bismuth species. According to [36], the UV–Vis spectrum for Bi_2O_3 shows a large absorption at ca. 400 nm. Therefore, the absence of peak at ca. 400 nm indicates that there is no bismuth oxide in the Bi-SBA-15 samples, and bismuth atoms enter the framework of Bi-SBA-15. This result is in agreement with the conclusion drawn from the Raman spectra.

The TG profile of the as-synthesized Bi-SBA-15 (B) is compared with that of the as-synthesized pure siliceous SBA-15, as shown in Fig. 6. Three regions of weight loss are observed in the temperature range 313–458, 458–488, and 488–1073 K for SBA-15 and in the temperature range 313–473, 473–553, and 553–1073 K for Bi-SBA-15 (B). The first weight loss [1.0 wt% for SBA-15 and 3.5 wt% for Bi-SBA-15 (B)] corresponds to the desorption of physically adsorbed water or ethanol. The second one is attributed to the decomposition of the organic template P_{123}. A weight loss (44.2 wt%) of P_{123} with decomposition temperature (T_d) around 458–488 K is observed on the pure siliceous SBA-15, which is consistent with the literature results [37]. As for Bi-SBA-15, the T_d of P_{123} (473–553 K) is apparently elevated, with a weight loss of 42.5 wt%. The higher T_d of the template in the as-synthesized Bi-SBA-15 (B), in comparison with that of the as-synthesized SBA-15, indicates that there might exist strong interactions between the bismuth species in the framework and the template. The third step weight loss [3.8 wt% for SBA-15 and 6.5 wt% for Bi-SBA-15 (B)] is due to the release of water formed from the condensation of the hydroxyl groups in the silica framework. The total weight loss is 52.5 wt% for Bi-SBA-15 (B) and 49 wt% for SBA-15, respectively.

3.2 Catalytic Oxidation of Cyclohexane

3.2.1 Solvent-free Liquid Phase Oxidation of Cyclohexane by Oxygen Over Bi-SBA-15 Catalysts

The catalytic performances of Bi-SBA-15 catalysts were investigated for cyclohexane oxidation at 413 K and 1.0 MPa O_2 in a solvent-free system, and the results are given in Table 2. GC-MS analysis indicates that the main by-products are adipic acid and some esters. SBA-15 is found to be inactive for cyclohexane oxidation under the above conditions. Hence, the excellent catalytic activity observed with Bi-SBA-15 arises from the presence of active bismuth sites in the catalysts. According to UV–Vis DRS, the active center is tetrahedral isolated Bi^{3+} ion in the SBA-15 mesoporous framework. Among the four catalysts, Bi-SBA-15 (B) (1.22 wt% bismuth) shows the best results with respect to the total yield of cyclohexanol and cyclohexanone (15.7%) after 4 h. While the bismuth content in the catalysts increased from 1.22 to 1.87 wt%, both the total yield of KA-oil and TOF value decreases. Furthermore, it is observed that the ratio of K/A increases with

Table 2 Cyclohexane oxidation over Bi-SBA-15 catalysts[a]

Catalyst	Conversion (mol%)	TOF[b] (h^{-1})	Selectivity (mol%)			K/A	Yield[c] (mol%)
			Cyclohexanol	Cyclohexanone	CHHP		
SBA-15	–	–	–	–	–	–	–
A	10.7	553	32	63	2.7	2.0	10.2
B	16.9	1339	19	74	1.8	3.9	15.7
C	13.4	1704	23	71	2.6	3.1	12.6
D	12.3	2530	27	66	2.3	2.4	11.4

[a] Reaction conditions: 8 mL cyclohexane, 40 mg catalyst, 413 K, 1.0 MPa O_2, 4 h, solvent-free system

[b] TOF, moles of cyclohexane converted per mole of bismuth in the catalyst per hour

[c] Yield, total yield of KA-oil

increasing conversion of cyclohexane. It might be attributed to the much higher activity of cyclohexanol, which could be oxidized to the more stable products such as cyclohexanone and adipic acid, with increasing activity of the catalyst in the systems.

Bi-SBA-15 (B) is employed to investigate the effect of different parameters on the oxidation of cyclohexane. The effect of reaction time over this catalyst is given in Fig. 7. With an increase in the reaction time, the conversion of cyclohexane and the selectivity to cyclohexanone increase, and the selectivity to cyclohexanol decreases. However, too long a reaction time leads to a decrease in the selectivity to cyclohexanone with a slight increase in the conversion of cyclohexane, thus the total yield of KA-oil decreases. Therefore, the appropriate reaction time is 4 h, with high total yield of KA-oil (15.7%). In addition, the selectivity to CHHP gradually decreases from 4.0 to 1.1 wt% with time.

Figure 8 illustrates the influence of reaction temperature. With increasing the reaction temperature, the conversion of cyclohexane increases. The selectivity to cyclohexanone also increases with reaction temperature up to 413 K at the expense of cyclohexanol. At higher reaction temperature, the selectivity to cyclohexanone decreases with a slight increase in the conversion of cyclohexane, thus the total yield of KA-oil decreases. Therefore, the appropriate reaction temperature is 413 K, with high total yield of KA-oil (15.7%).

The influence of oxygen pressure on cyclohexane oxidation is given in Fig. 9. An increase in oxygen pressure helps to increase the conversion of cyclohexane and the selectivity to cyclohexanone. Meanwhile, the selectivity to cyclohexanol decreases and at 1.4 MPa a decreased total yield of KA-oil is also noted.

The influence of the catalyst dosage on cyclohexane oxidation is given in Fig. 10. An increase in catalyst

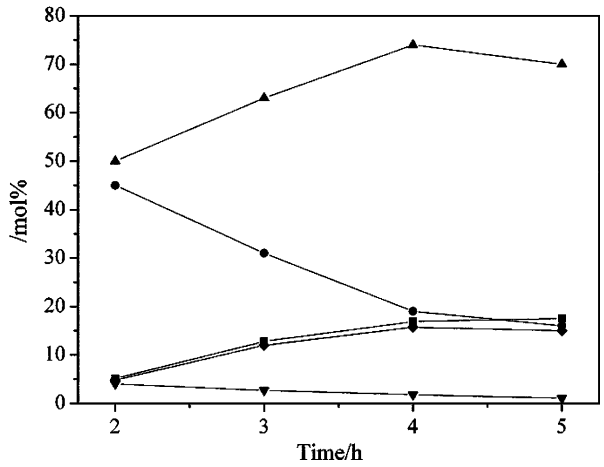

Fig. 7 Effect of reaction time on cyclohexane oxidation over Bi-SBA-15 (B). (Reaction conditions: 8 mL cyclohexane, 40 mg catalyst, 413 K, 1.0 MPa O_2, solvent-free system. ■: conversion of cyclohexane; ●: selectivity to cyclohexanol; ▲: selectivity to cyclohexanone; ▼: selectivity to CHHP; ◆: total yield of KA-oil.)

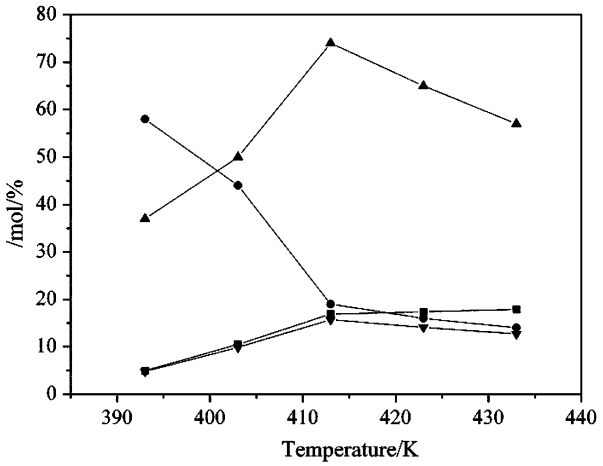

Fig. 8 Effect of reaction temperature on cyclohexane oxidation over Bi-SBA-15 (B). (Reaction conditions: 8 mL cyclohexane, 40 mg catalyst, 1.0 MPa O_2, 4 h, solvent-free system. ■: conversion of cyclohexane; ●: selectivity to cyclohexanol; ▲: selectivity to cyclohexanone; ▼: total yield of KA-oil.)

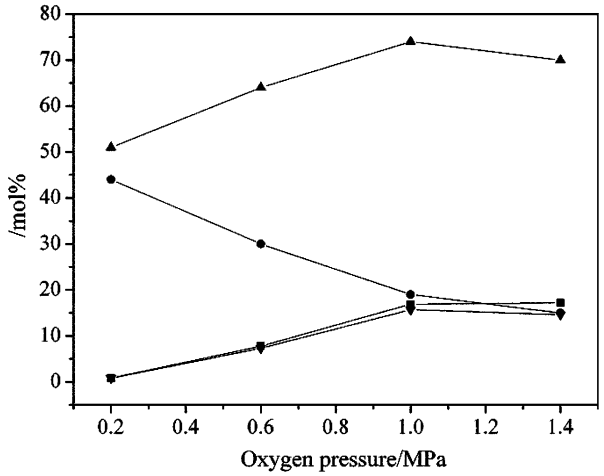

Fig. 9 Effect of oxygen pressure on cyclohexane oxidation over Bi-SBA-15 (B). (Reaction conditions: 8 mL cyclohexane, 40 mg catalyst, 413 K, 4 h, solvent-free system. ■: conversion of cyclohexane; ●: selectivity to cyclohexanol; ▲: selectivity to cyclohexanone; ▼: total yield of KA-oil.)

dosage helps to increase the conversion of cyclohexane. The selectivity to cyclohexanone is almost constant, and the selectivity to cyclohexanol decreases. While the catalyst dosage is beyond 40 mg, the total yield of KA-oil decreases.

Recycling tests were performed using Bi-SBA-15 (B) under the typical reaction conditions. After the reaction was finished, the catalyst was separated by filtration from the reaction mixture, washed with acetone, dried, and reused in the next catalytic run. As shown in Fig. 11, after the catalyst is used repeatedly four times, the conversion and the selectivity to KA-oil are well retained. This analysis confirms the stability and recyclable applicability of Bi-SBA-15 for the oxidation of cyclohexane with O_2 in a solvent-free system.

In order to ensure the possibility of radical reaction mechanism, a small amount of radical initiator (TBHP) was added. As shown in Table 3, the conversion of cyclohexane was increased from 16.9 to 23.4% retaining the total

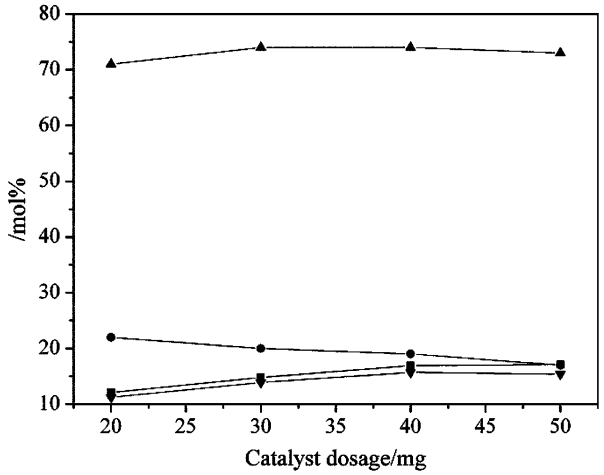

Fig. 10 Effect of the dosage of Bi-SBA-15 (B) on cyclohexane oxidation. (Reaction conditions: 8 mL cyclohexane, 413 K, 1 MPa O_2, 4 h, solvent-free system. ■: conversion of cyclohexane; ●: selectivity to cyclohexanol; ▲: selectivity to cyclohexanone; ▼: total yield of KA-oil.)

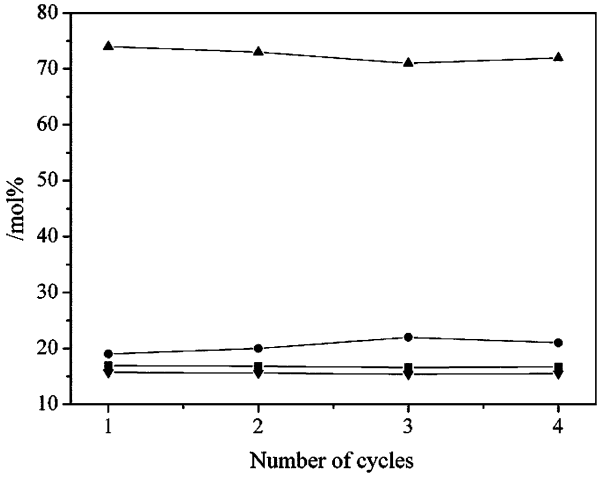

Fig. 11 Recycling studies performed over Bi-SBA-15 (B). (Reaction conditions: 8 mL cyclohexane, 40 mg, 413 K, 1.0 MPa O_2, 4 h for one cycle, solvent-free system. ■: conversion of cyclohexane; ●: selectivity to cyclohexanol; ▲: selectivity to cyclohexanone; ▼: total yield of KA-oil.)

Table 3 Effect of TBHP or HQ on the cyclohexane oxidation over Bi-SBA-15 (B)[a]

Catalyst	Conversion (mol%)	TOF[b] (h^{-1})	Selectivity (mol%)		K/A	Yield[c] (mol%)
			Cyclohexanol	Cyclohexanone		
B	16.9	1,339	19	74	3.9	15.7
B[d]	23.4	1,854	22	70	3.2	21.5
B[e]	3.2	254	16	76	4.8	2.9

[a] Reaction conditions: 8 mL cyclohexane, 40 mg catalyst, 413 K, 1.0 MPa O_2, 4 h, solvent-free system

[b] TOF, moles of cyclohexane converted per mol of bismuth in the catalyst per hour

[c] Yield, total yield of KA-oil

[d] Reaction carried out in presence of TBHP (3 wt% of cyclohexane)

[e] Reaction carried out in presence of HQ (3 wt% of cyclohexane)

Table 4 The comparison of Bi-SBA-15 with other reported redox molecular sieves for cyclohexane oxidation

Catalyst	Reaction conditions	Conv/mol%	Sel/mol%		Yield[a]/mol%	References
			nol	none		
Bi-SBA-15(B)	413 K, 1MPa O_2, 4 h	16.9	19	74	15.7	This work
FeAlPO-5	403 K, 1 MPa air, 8 h	2.5	41.1	17.9	1.5	[11]
	403 K, 1 MPa air, 24 h	6.6	36.2	15.5	3.4	
MnAlPO-5	403 K, 1 MPa air, 8 h	2.7	36.9	56.0	2.5	[11]
	403 K, 1 MPa air, 24 h	6.2	18.5	42.8	3.8	
CoAlPO-5	403 K, 1 MPa air, 8 h	1.6	35.0	21.7	0.9	[11]
	403 K, 1 MPa air, 24 h	2.0	15.0	67.8	1.6	
Au/ZSM-5	423 K, 1 MPa O_2, 4 h	16	26	66	14.7	[12]
Ce/AlPO-5	413 K, 0.5 MPa O_2, 4 h	13	40	51	11.8	[13]
Co/ZSM-5	373 K, 1 MPa O_2, 4 h	7.5	46	46.4	6.9	[14]
Fe/AlPO	403 K, 2 MPa air, 24 h	7.5	86.6	7.0	7.0	[15]
[Cr]MCM-41	388 K, 1 MPa O_2, 6 h	<10	~20	~70	<9	[16]
[Cr]MCM-48	388 K, 1 MPa O_2, 6 h	<10	~20	~70	<9	[16]
Bi-MCM-41	423 K, 1 MPa O_2, 4 h	17	19	72	15.5	[17]
$C_{27}ClC_{15}$[b]	393 K, 2.7 MPa air, 6 h	8.0	29	63	7.4	[18]
Au/MCM-41	423 K, 1 MPa O_2, 6 h	19	21	73	17.9	[19]
Au/SBA-15	423 K, 1 MPa O_2, 6 h	18	18	75	16.7	[20]

[a] Yield, total yield of KA-oil

[b] $C_{27}ClC_{15}$, Chromium-containing small pore mesoporous silica

selectivity to cyclohexanol and cyclohexanone. When the reaction was carried out in the presence of radical inhibitor (HQ), a decrease in the cyclohexane conversion to 3.2% was observed. These results confirm the radical initiated mechanism.

3.2.2 *The Comparison of Bi-SBA-15 with Other Reported Catalysts for Cyclohexane Oxidation*

In recent years, there are some reports on using other redox molecular sieves as catalyst for this reaction, such as metal heteroatom (Fe, Mn, Co, or Ce)-containing aluminophosphate [11, 13, 15], Au/ZSM-5, Co/ZSM-5 [12, 14], metal heteroatom (Cr, Bi, or Au)-containing MCM-41, MCM-48, or small pore mesoporous silica [16–19], and Au/SBA-15 [20]. As shown in Table 4, the KA-oil yield of lower than 15.7% is obtained while using most of these catalysts. Au/MCM-41 [19] and Au/SBA-15 [20] are very efficient for this reaction, with a KA-oil yield of 17.9 and 16.7%, respectively. However, gold is a noble metal and its extensive application would be seriously limited. Compared with these catalysts, it could be found that Bi-SBA-15 is an excellent and cheaper catalyst for the selective oxidation of cyclohexane by oxygen.

4 Conclusion

We have demonstrated the first synthesis and characterization of bismuth-containing SBA-15 mesoporous molecular sieves, prepared by a direct hydrothermal method. XRD patterns indicate that the synthesized materials have an ordered 2D *p6mm* hexagonal mesostructure. The unit-cell parameter of Bi-SBA-15 materials increases with an increase in the content of bismuth incorporated in the framework. Raman spectroscopy and UV–Vis DRS show that bismuth atoms in Bi-SBA-15 exist in a highly dispersed state. In the catalytic test, Bi-SBA-15 is found to be an efficient and reusable catalyst for the oxidation of cyclohexane, in a solvent-free system, with oxygen as oxidant. In the condition of 1 MPa O_2 and 413 K for 4 h, the conversion of cyclohexane is 16.9%, and the total selectivity of cyclohexanol and cyclohexanone is 93%. Different parameters have an evident influence on the catalytic performances.

References

1. Berezin IV, Denisov ET, Emanuel NM (1968) Oxidation of cyclohexane. Pergamon, New York
2. Chandalia SB (1977) Oxidation of hydrocarbons, 1st edn. Sevak, Bombay

3. Barton DHR, Bévière SD, Hill DR (1994) Tetrahedron 50:2665
4. Vanoppen DL, De Vos DE, Genet MJ, Rouxhet PG, Jacobs PA (1995) Angew Chem Int Ed Eng 34:560
5. Zhou L, Xu J, Miao H, Wang F, Li X (2005) Appl Catal A: Gen 292:223
6. Tong J, Li Z, Xia C (2005) J Mol Catal A: Chem 231:197
7. Guo C, Chu M, Liu Q, Liu Y, Guo D, Liu X (2003) Appl Catal A: Gen 246:303
8. Guo C, Huang G, Zhang X, Guo D (2003) Appl Catal A: Gen 247:261
9. Huang G, Guo C, Tang S (2007) J Mol Catal A: Chem 261:125
10. Huang G, Guo Y, Zhou H, Zhao S, Liu S, Wang A, Wei J (2007) J Mol Catal A: Chem 273:144
11. Raja R, Sankar G, Thomas JM (1999) J Am Chem Soc 121:11926
12. Zhao R, Ji D, Lv G, Qian G, Yan L, Wang X, Suo J (2004) Chem Commun 904
13. Zhao R, Wang Y, Guo Y, Guo Y, Liu X, Zhang A, Wang Y, Zhan W, Lu G (2006) Green Chem 8:459
14. Yuan H, Xia Q, Zhan H, Lu X, Su K (2006) Appl Catal A: Gen 304:178
15. Subrahmanyam C, Viswanathan B, Varadarajan TK (2004) J Mol Catal A: Chem 223:149
16. Laha SC, Gläser R (2007) Micro Meso Mater 99:159
17. Qian G, Ji D, Lv G, Zhao R, Qi Y, Suo J (2005) J Catal 232:378
18. Shylesh S, Samuel PP, Singh AP (2007) Appl Catal A: Gen 318:128
19. Lv G, Zhao R, Qian G, Qi Y, Wang X, Suo J (2004) Catal Lett 97:115
20. Lv G, Ji D, Qian G, Qi Y, Wang X, Suo J (2005) Appl Catal A: Gen 280:175
21. Zhao D, Feng J, Huo Q, Melosh N, Fredrickson GH, Chmelka BF, Stucky GD (1998) Science 279:548
22. Selvaraj M, Kawi S (2007) Chem Mater 19:509
23. Selvaraj M , Lee TG (2006) J Phys Chem B 110:21793
24. Vinu A, Srinivasu P, Miyahara M, Ariga K (2006) J Phys Chem B 110:801
25. Wu S, Han Y, Zou Y, Song J, Zhao L, Di Y, Liu S, Xiao F (2004) Chem Mater 16: 486
26. Vinu A, Sawant DP, Ariga K, Hossain KZ, Halligudi SB, Hartmann M, Nomura M (2005) Chem Mater 17:5339
27. Chen S, Jang L, Cheng S (2004) Chem Mater 16:4174
28. El Berrichi Z, Louis B, Tessonnier JP, Ersen O, Cherif L, Ledoux MJ, Huu CP (2007) Appl Catal A: Gen 316:219
29. Jarry B, Launay F, Nogier JP, Montouillout V, Gengembre L, Bonardet JL (2006) Appl Catal A: Gen 309:177
30. Li C, Wang Y, Guo Y, Liu X, Guo Y, Zhang Z, Wang Y, Lu G (2007) Chem Mater 19:173
31. Vinu A, Murugesan V, Böhlmann W, Hartmann M (2004) J Phys Chem B 108:11496
32. Luan Z, Bae J, Kevan L (2000) Chem Mater 12:3202
33. Shulpin GB, Attanasio D, Suber L (1993) J Catal 142:147
34. Newalkar BL, Olanrewaju J, Komarneni S (2001) Chem Mater 13:552
35. Morey MS, Stucky GD, Schwarz S (1999) J Phys Chem B 103:2037
36. Xie J, Lu X, Chen M, Zhao G, Song Y, Lu S (2007) Dyes Pigm XX:1
37. Zhao D, Huo Q, Feng J, Chmelka BF, Stucky GD (1998) J Am Chem Soc 120:6024